Hindawi
Advances in Materials Science and Engineering
Volume 2022, Article ID 1667041, 11 pages
https://doi.org/10.1155/2022/1667041

Research Article

Investigation of Friction Stir-Welded B_4C Particles-Reinforced Copper Joint: Mechanical, Fatigue, and Metallurgical Properties

M. Vetrivel Sezhian,[1] G. Chakravarthi,[1] K. Giridharan,[1] Balasubramaniam Stalin,[2] B. Yokesh Kumar,[3] P. Sureshkumar,[4] J. Vairamuthu,[5] and Ramaswamy Krishnaraj[6,7]

[1]*Department of Mechanical Engineering, Easwari Engineering College, Chennai 600089, Tamil Nadu, India*
[2]*Department of Mechanical Engineering, Anna University, Regional Campus Madurai, Madurai 625 019, Tamil Nadu, India*
[3]*Department of Mechanical Engineering, Chennai Institute of Technology, Chennai, Tamil Nadu, India*
[4]*Department of Mechanical Engineering, Ramco Institute of Technology, Rajapalayam 626117, Tamil Nadu, India*
[5]*Department of Mechanical Engineering, Sethu Institute of Technology, Pulloor 626 115, Kariapatti, Tamil Nadu, India*
[6]*Centre for Excellence-Indigenous Knowlegde, Innovative Technology Transfer and Enterpreneurship, Dambi Dollo University, Dambi Dollo, Ethiopia*
[7]*Department of Mechanical Engineering, Dambi Dollo University, Dambi Dollo, Ethiopia*

Correspondence should be addressed to Ramaswamy Krishnaraj; dr.krishnarajdirectorcei@dadu.edu.et

Received 12 October 2021; Revised 26 November 2021; Accepted 23 February 2022; Published 11 March 2022

Academic Editor: Zhiping Luo

Solid-state friction stir welding (FSW) is a sophisticated technique that can join materials that are similar and different without significantly affecting the properties of the base materials. The purpose of this study is to enhance the tensile strength, micro-hardness, and fatigue strength of the copper (C1100) butt-joints reinforced with B_4C nanoparticles. The effects of B_4C nano-particle inclusion on the mechanical properties of the fabricated joints are studied in correlation with the microstructural features of the welded joints using optical microscopy. The joints are fabricated on a specialized friction stir welding machine (VMC-TC-1200) with a square pin-profiled tool. Defect-free joints of 3 mm copper plates are produced at the constant tool rotational speed of 1100 rpm, welding speed of 30 mm/min, plunge depth of 0.25 mm, and constant axial stress of 5 kN. B_4C particles of 1, 2, 3, and 4wt% are added to the joints and their properties are compared with the joints produced without the inclusion of B_4C particles to study the effects of the addition of nanoparticles. The joints attained a maximum micro-hardness of 123 HV, fatigue strength of 159 MPa, and tensile strength of 203 MPa with the addition of 3% B_4C. Microstructural investigations performed through an optical microscope and scanning electron microscope (SEM) indicated the presence of homogeneously distributed B_4C particles engulfed by finely refined grains. The thermal conductivity of the B_4C particles facilitated the smooth flow of copper around the particles by forming a thin lubricating layer, thus improving the properties of the joints. Furthermore, this study has established that the addition of B_4C particles is an effective and eco-friendly method of producing strong joints which could be used for industrial and defense applications.

1. Introduction

FSW is a promising approach for producing automobile components, as well as used in aerospace and space technology. This technique is one of the best and simple methods for joining aluminum, copper, and its alloys, and it also offers the potential to join even higher temperature materials such as steel. The nonconsumable rotating tool is used to connect alloys that are similar and different in composition. Under various axial load conditions, the FSW rotating tool creates frictional heat between the abutting edges, converting mechanical energy into heat energy without employing electrical energy to form the weld substance. This method is frequently utilized to produce quality joints in nonferrous alloys [1–3]. The heat generation and plastic deformation were analyzed during friction stir lap welding

of aluminum alloy, and mild steel rotational speed, welding speed, and tool design were investigated on the weld joint structure of Al-steel [4]. A special welding tool was used in the FSW of copper. Copper (Cu) welding joint was tested under metallographic analysis, mechanical testing, and X-ray inspection. Copper alloys, being one of the most important lightweight structural materials, have excellent strength characteristics alloys. It has recently been mixed with different steel alloys and aluminum materials for different applications. The dissimilar joints produced from FSW are used for aerospace applications [5–7]. Defect-free welded joints were produced in Cu and steels by FSW using different tool shoulder diameters. They have good strength, density, thermal conductivity, corrosion resistance, machinability, and nonmagnetic properties [8, 9]. The effects of the tilt angle on the parameters of dissimilar FSW copper to aluminum were investigated. The different FSW parameters and tool designs were used to achieve better-welded joints using Al-Cu [10, 11].

The impact of the FSW parameters on the mechanical properties of copper-welded joints and their microstructural characteristics has been studied. The applications of copper alloys have increased significantly in recent years due to their superior material and thermal properties. The FSW process has a number of advantages, including the ability to weld without melting the base material. Hence, this process exhibits reduced welding defects such as porosity and internal cracks [12–14]. The thermal behaviors and the defects of the friction stir-welded dissimilar copper and steel joints have been analyzed. The tool rotational speed and linear speed were the most influential parameters to decide the weld joint quality of the copper-steel joints [15]. The physical properties and the microstructure of the welded joints differ based on the heat input, rotational speed of the pin, and the nature of the materials. In the friction stir welding process, different process factors such as pin profiles, feed rate, tool rotational speed, the gap between the tool and the workpiece, and welding speed are varied. Friction stir welding is an attractive technique for joining different alloys in solid-state conditions without any defects. Friction stir-welded dissimilar joints are used for various applications in automobile and aerospace sectors [16–19]. The effects of various FSW input factors on the behavior of the dissimilar Al-Cu joints were investigated. The plunge depth and the forging action of the tool play an important role in the generation of heat during the material joining process, which in turn affects the consolidation of the joint [20]. Based on the literature reviewed, there is no significant work on the FSW process-optimized tool speed, welding speed, and various weight percentages addition of boron carbide (B_4C) particles-reinforced copper alloy weld joints.

The primary goal of this work is to investigate the effects of boron carbide particulates on the microstructure and the mechanical properties of the friction stir-welded C1100 alloy joints. Boron carbide particles were added at 1%, 2%, and 3% by weight for fabricating the composite weld joints. The microstructural studies conducted using SEM indicated significant grain refinement in the nugget zone (NZ) of the joints containing 3% B_4C. Instances of nucleations around the B_4C particles and piling of the particles around the grain boundaries were also noticed. The B_4C particles acted as nucleating sites causing significant grain refinement. This is in good agreement with the findings reported in the welding of B_4C-doped AA7075 friction stir-welded joints by Vijaya Kumar et al. [21]. Microstructural studies were utilized to good agreement with the tensile strength and micro-hardness results. Through this study, it is confirmed that the addition of B_4C particles improved the microstructural and the mechanical properties of the copper alloy joints. This technology could be used in the construction of armor tanks and other defense applications.

2. Experimental Methods

2.1. Materials. C1100 copper alloy plates with a 3 mm thickness were selected for this present investigation. As a result of its corrosion resistance, high electrical and thermal conductivity, and esthetically pleasing appearance, it is a very versatile alloy. The copper plates were cut to a length of 100 mm and a width of 50 mm for the purpose of this project. Electric discharge machining was used to drill an array of 40 cylindrical holes (20 numbers on each sheet) with a diameter of 1 mm and a depth of 1.5 mm on the faying surface (abutting edges) at an equal distance of 5 mm. This was done in order to incorporate the B_4C particles in the nugget zone for FSW, and the holes were drilled at an equal distance of 5 mm using electrical discharge machining (EDM). Cleansing acetone solution was used to gently degrease all copper sheets before they were allowed to dry in open air. The estimated density of the boron carbide slurry in the drilled holes was 2.8 g/mm^3, based on the size of the holes and the number of holes. The chemical composition of the base material copper (C1100) alloy is listed in Table 1. A nonconsumable FSW tool consisting of a shank, shoulder, and probe is employed. Several types of researches have demonstrated that flat, concave, and convex form shoulders are better to heat due to their nature in the FSW process. The form of the tool pin has a significant influence on weld joint integrity. In the current investigation, the B_4C-reinforced copper weld joints were constructed using square tool pin profiles with flattened shoulders. The tool, which was constructed of high-carbon, high-chromium steel and had a square head pin profile, was used to manufacture weld joints. It had been oil hardened to 63–64 HRC and had a square head pin profile. Figure 1 is a schematic representation of the boron carbide particles used in this investigation. The mechanical and thermal characteristics of the copper (C1100) alloy are tabulated in Table 2.

2.2. Joint Fabrication Process. Friction stir welding was performed by a specialized friction stir welding machine (VMC-TC-1200), which is capable of producing a maximum downward force of 8 kN. The tool profile for the FSW featured a cylindrical shoulder with a diameter of 20 mm and a pin profile (square head) with pin length of 2.85 mm, sides

Table 1: Chemical compositions of the copper (C1100) alloy in wt%.

Elements	Zn	Pb	Sn	P	Fe	Ni	Cr	Al	S	As	Bi	Balance
Copper (C1100)	0.209	0.011	0.031	0.018	0.089	0.023	0.005	0.009	0.011	0.005	0.004	Cu

(a) (b)

Figure 1: Schematic view of the boron carbide particles and the FSW tool.

Table 2: Thermal and mechanical properties of the copper (C1100) alloy.

Base metal	Hardness (HV)	Ultimate tensile strength (MPa)	% of elongation	Yield strength (MPa)	Thermal conductivity (W/mK)
Copper (C1100)	135	225	23	104	388

of 3 mm × 3 mm, and 9 mm^2 area, respectively. FSW was done as the butt joint method using constant tool rotating speed at 1100 rpm, and the transverse velocities were 30 mm/min. The tool's tilt was set to 0 degrees, while the depth of the plunge was 0.25 mm and the dwell duration was 6 seconds. These were the reference process parameters that were maintained in accordance [22–24]. Figure 2(a) depicts the experimental setup used in this study. Figure 2(b) shows before and after welded B_4C-reinforced copper joints that are similar metals. For all the weld samples, a single FSW pass was employed. The B_4C wt% and other process parameters were maintained constant. Table 3 shows the weight percentage of B_4C designations that were used in the FSW weld joints' fabrication process. The joint quality, surface appearance, cracks, weld flash, and cavities of the weld joints with B_4C particles-assisted weld joints were inspected after the joining process.

2.3. Test Sample Preparation. The abrasive water jet machining was used to cut the visually examined copper C1100-welded samples in accordance with ASTM requirements. It was necessary to maintain the process parameters of 320 psi water pressure, garnet size of 80 mesh, 0.35 kg/min abrasive flow rate, and nozzle diameter of 1 mm. To avoid mode I shear failure, the machined specimens were polished with 320 grit abrasive paper at the ends and curves to smooth the edges [25].

3. Characterization

The cross-sectional surface of the welds was machined prior to tensile testing to minimize the rough impressions on the surface. Universal testing equipment with a 40 Ton loading capacity was used to examine the tensile characteristics of friction stir-welded B_4C particles-aided copper identical plates, which were tested in accordance with ASTM E8-04 standards. When the crosshead was moving at a speed of 2 mm/min, the load-displacement relationship was displayed on the X-Y graph. The hardness of the weld samples was determined using a Vickers hardness tester, which was then tested in accordance with ASTM 384. Using 200 g of force for 15 seconds, micro-hardness testing was carried out at a depth of 1 mm below the top surface throughout the nugget zone, with a minimum of 5 locations examined in order to calculate the average hardness. The fatigue strength of similar B_4C-aided copper-welded connections was examined in the same manner using a tensile fatigue tester. The specimens for the fatigue tests were produced in line with the ASTM standard. During these investigations, a hydraulic test machine from MTS Instron with a load cell of 50 kN was used to simulate fatigue test machines. Throughout the trial, the process parameters for the fatigue test were 10 Hz, 0.1 stress ratio, and 23°C working temperature. The fatigue strength of the test specimen was calculated after 10^7 cycles at 50% of the ultimate tensile stress of the sample. With the use of an optical microscope,

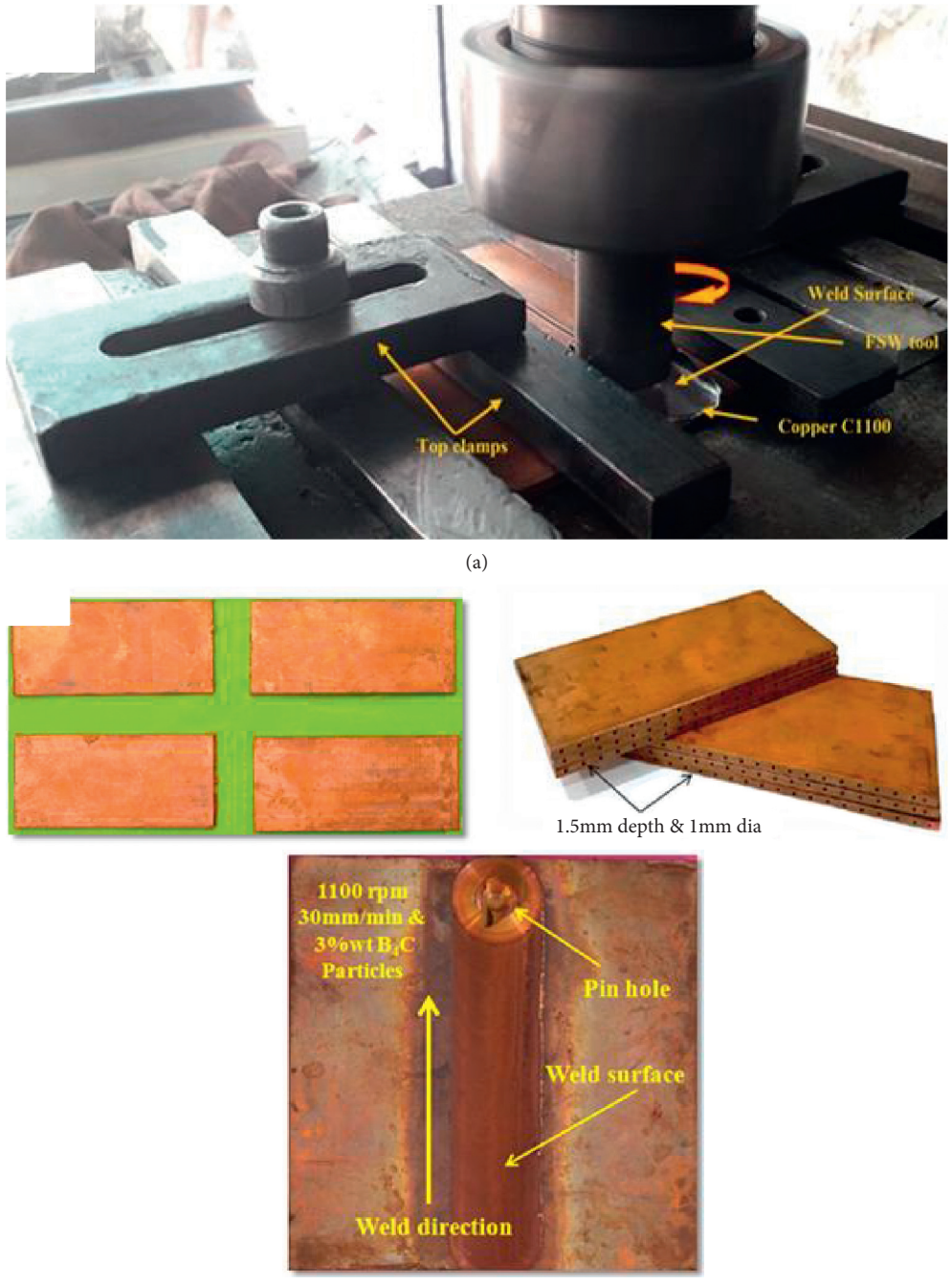

Figure 2: (a) Photographic view of the FSW process with inclusion of B_4C particles. (b) Before and after welded samples.

the macro and microstructures of the weld joints were investigated (DE-Winto Inverted Trinocular, Version -2). The samples were ground using a succession of abrasive sheets with grit sizes ranging from 60 to 5/0 (US system). The diamond fine abrasives were utilized for mirror polishing, and then the colloidal alumina paste was employed to finish the job. For the purpose of exposing the grain structure, potassium dichromate and Keller solution were used as etching agents, and photographs were taken using polarized light. A field emission electron microscope was used to examine the microscope pictures of the weld nuggets and fractography analyses were examined (FEI, QUANTA). The elemental mapping features of this FESEM are also included.

4. Results and Discussion

4.1. Mechanical Properties. Table 4 displays the tensile strength, percentage of elongation, yield strength, and maximum strain experience of the weld beads. The tensile strength of the unfilled B_4C particles copper weld was 168 MPa, the yield strength was 138 MPa, the percentage of

Table 3: FSW welds with B_4C designation.

Weld designation	wt% of B_4C added
C-C	0
C-C_1	1
C-C_2	2
C-C_3	3
C-C_4	4

C-C: copper-copper.

Table 4: Mechanical properties of the FSW welds.

Weld designation	Tensile strength (MPa)	% of elongation	Yield strength (MPa)	Maximum strain (%)
C-C	168	17	138	26
C-C_1	179	27	149	30
C-C_2	181	35	157	34
C-C_3	203	44	177	37
C-C_4	183	38	161	32

elongation was 17, and the maximum strain value was 26. The measured mechanical characteristics suggest a weld joint efficiency of about 60%. The speed of the rotating tool causes increased brittleness in the stir zone, reducing joint efficiency. The grain was significantly deformed and maintained higher thermal and mechanical stress due to the fast cooling of the base metal in the welding zone [2, 14, 26].

The inclusion of the B_4C particles of a substantial volume enhanced the mechanical characteristics and joint efficiency by around 74%. The B_4C-aided weld designations C, C-C1, C-C2, C-C3, and C-C4 showed increases in tensile strength of 8%, 13%, 19%, and 12%, yield strength of 9%, 17%, 24%, and 11%, percentage of elongation of 31%, 49%, 59%, and 53%, and maximum strain of 13%, 24%, 28%, and 21%. The efficient lubricating and strengthening actions of boron carbide particles are responsible for this improvement. Because B_4C particles have high thermal conductivity, they transfer the heat generated during stirring, reducing the thermally and thermomechanically impacted zones. The heat produced by the pores in the B_4C structure is balanced and kept in the air-filled gaps, resulting in a more comfortable environment. A thin lubricating layer between the sliding surfaces is produced during mixing, which refines the plastically deformed grain and helps reduce the amount of thermally damaged grain. As a consequence, the ductility and elongation of the weld nugget were maintained, which enhanced the tensile characteristics of the weld nugget [27]. Furthermore, because of the high rotational speed of the tool, the addition of B_4C finely disperses in the stir zone, resulting in a change in the microstructure. The nucleation action is enhanced by the presence of boron particles, resulting in the formation of additional intermetallic phases. These phenomena enhanced the mechanical characteristics of the weld generated by the FSW technique. However, a high dosage of boron particles in the weld section, up to 4wt %, has a minor impact on weld strength. In the matrix, the super-saturated B_4C particles clump together and create a thick lubricating layer. As a result, the frictional heat generated between the workpiece and the tool is insufficient to deform and join plastically. Adding boron particles to the weld process increased the weld quality and reduced stress. Figure 3 depicts different FSW joints by tension-fractured samples.

As shown in Figure 3(a), the friction stir welding process produced a clean copper and copper connection with the addition of B_4C particles, which was achieved by utilizing the friction stir welding method. On the retreating side of the joint, a fracture at the TMAZ showed enhanced brittleness due to high frictional heat and mechanical plunging pressure during retreating. Because of the larger grains, the HAZ portion on both the retreating and advancing sides was weaker than the rest of the segment. Similarly, the FSW joints C-C1 and C-C2 are shown in Figures 3(b) and 3(c), respectively. B_4C particles, which are present in just a trace quantity, reduce the likelihood of heat-affected grains forming in the HAZ area by a minuscule percentage when present. The solid lubricant between the spinning surfaces supplied adequate sliding force while also preventing the production of excess heat between the moving surfaces. This examination indicates that the weld area of all weldments has evenly dispersed B_4C particles at the nugget region. With an addition of 3wt% of B_4C particles, the tensile strength and yield strength of the weld joints reached the maximum as shown in Figure 3(f). High heat is the main cause of fracture on the retreating side, and may have caused the grain size to increase. The fracture, on the other hand, occurred in the center of the nugget in Figures 3(d) and 3(e). Because of the finer grains and the absence of varied heat flow on both the advancing and retreating sides, the fracture occurred in the middle. As the central nugget can withstand bigger grains, the fracture can eventually cleave. Figure 4 depicts a graphical representation of the Vickers hardness of welded joints. Vickers hardness of the center nugget of the weld shape is determined to be the highest of all the nuggets tested. The unfilled B_4C particles copper similar weld was found to have the greatest hardness of 123 HV. The fine mixing of boron particles and copper atoms and fast cooling at the nugget zone is the source of the higher value. The quenching action in the stir zone is improved by fast cooling, thus enhancing the hardness of the joints due to the development of a finer grain structure. Hardness was maintained less in the thermomechanically treated (TMT) and

Figure 3: Fractured tensile samples.

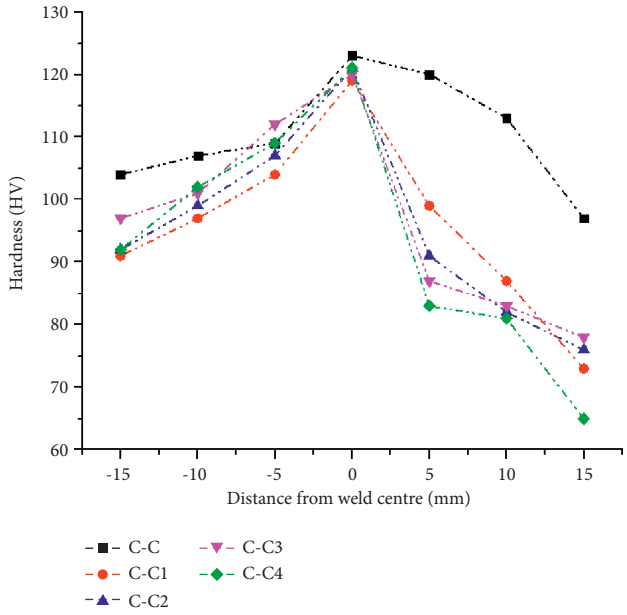

Figure 4: Hardness analysis in different zones.

thermally affected zones compared to the nugget. On the other hand, the hardness has improved.. It is believed that distracted (slow) cooling is responsible for this increase in hardness, which results in thermomechanically treated grains as well as thermally deformed grains in the TMT and HAZ. It is noticed that the lubricant effect lowers the TMT and HAZ effects with additional B_4C additions of substantial volume. Thermally changed grains and other oxide reactions are less likely when boron carbide particles effectively control heat. The thermomechanical action is limited by the impact of solid lubrication, which decreases thermal stress in mixed grains while simultaneously maintaining the absorption of the generated heat. At the nugget zone, the drop in hardness is 4%, 9%, 14%, and 3%, respectively. The TMT and HAZ also showed similar decrements. As a result, the inclusion of boron particles balanced the heat development and kept the grains from becoming thermally exhausted. Nevertheless, it should be mentioned that adding more B_4C than 2wt% enhanced the hardness even more. A supersaturated mix resulted from the increased volume of B_4C particles deposited in the copper-copper contact. As a result of the increased heat rejection, the grains become finer, resulting in increased hardness [28–30]. Rather than grain size, the hardness of the FSW copper weld zone was determined by the density of dislocations. Due to temperature and mechanical conditions, there is a hardness difference in the stir zone from the upper to the lower region.

5. Fatigue Behavior Analysis

The fatigue strength of different weld beads reinforced with and without boron carbide particles is shown in Figure 5. According to the manufacturer, the bare copper-copper weld has a nominal fatigue strength of 117 MPa. During fine stirring and rapid cooling of heat-affected zones, this lower value produces extremely brittle mixed copper and boron carbide particles. This fast cooling produced finer grains in the HAZ and TMT zones, and fine equiaxed crystals in the welded area. As a consequence, the fatigue strength is given a lower value. It was found that by introducing boron carbide particles in modest concentrations of 1, 2, and 3wt% to the weld zone, the fatigue strength was immediately increased. The purpose of this modification is to increase the fatigue strength of the weld beads in order to reach 10^7 cycles. This increase in fatigue strength is the result of two factors. First, the presence of B_4C particles inhibits the development of thermally deformed grains by removing the heat generated in the stir zone; as a consequence, the generation of finer grains is substantially decreased while the size of the coarse grains is maintained. The boron carbide particles serve as a strong lubricant throughout the welding process and help maintain a suitable cooling rate, resulting in big grains in the TMT and HAZ sections and relatively small grains in the nugget [31]. The second is the impact of the carbon in the weld zone on the overall strength of the weld. Carbon in the stir zone fills in the gaps produced by the flow of mixed materials and ensures that the weight is carried in a

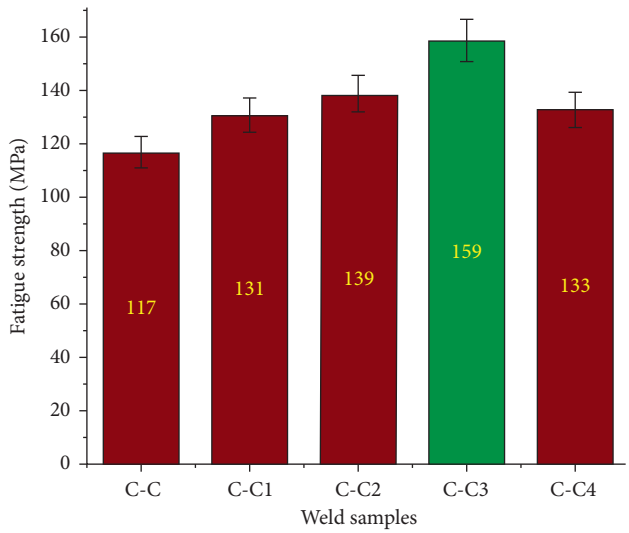

Figure 5: Fatigue strength of the weld samples.

consistent manner. Smaller surface discontinuities and finer carbon enhance the homogeneity of the weld nuggets, resulting in a stronger weld nugget by decreasing the stress intensity factor in the weld nuggets. When a large amount of B_4C particles is present, it has been shown that the fatigue strength has reduced. Because of the super-saturated carbon atoms present in the copper intermetallic mix, the fatigue strength is reduced to a bare minimum. Additional boron carbide particles produced a thick precipitate in the weld zone, which interfered with heat transmission and load-bearing. The high carbon concentration in the nugget zone also results in a weld bead with low hardness and increased brittleness, which is undesirable. As a result, a little reduction in fatigue strength was seen.

6. Microstructure Analysis

The microstructures of copper identical welded joints produced by the boron carbide-aided friction stir welding technique were examined using an optical microscope, and the relevant micrographs are presented in Figure 6. Following that, the weld samples were etched for 20 seconds in potassium dichromate solution to show the microstructure and associated properties. Following that, optical microscopy was used to characterize the microstructural evolutions as well as the well-fractured surfaces of the samples. The microstructure study revealed that as the heat input increases, so does the size of the fragmented copper and B_4C particles, and that altering the process parameters and tool pin profile results in a substantial change in the dispersion of copper particles. The microstructure of the copper alloy utilized in this investigation is shown in Figure 6(a). The microstructure of the copper plates with big equiaxed copper grains and precipitated cuprous oxide at the grain boundaries with irregular borders is shown. The grain size of copper is in the range of 30 microns. The matrix also shows twinned areas with parallel lines, and the cold formation of the sheet demonstrated the ductility. Figure 6(b) depicts the copper and copper weld contact. The grain structure around the weld zone differed significantly from that of the substrate. SZ were distinguished by their fine and equiaxed grain structure, whilst HAZ were distinguished by their grain growth. However, even though the grain size of the weld zone was comparatively smaller, it caused a tiny softening region in the weld zone. Twinned grains and the presence of cuprous oxide discovered at the interface of copper grain boundaries indicate the soundness in the joint interface. Grain fragmentation is shown in Figure 6(c), which shows the copper nugget zone. Copper granules have a diameter of about 20 microns and include minute recrystallized grains. It is possible that these tiny recrystallized grains are responsible for the fast cooling and enhanced hardness of the stir zone [32, 33].

Figure 6(d) depicts a boron carbide particle that was found in the nugget zone in a similar vein. The particles were evenly distributed and adhered to the surface of the substrate. Copper nugget zone fractures result in the production of tiny recrystallized grains of B_4C particles in the copper nugget zone. As additional precipitates are formed in the matrix phase, the number of boron carbide particles increases as a nucleation agent is used by each particle. Due to this, the initiation of cracks in the matrix decreased, which resulted in an improvement in the tensile and fatigue strength, respectively. It was also observed that copper particle colloids were penetrated. Figure 6(e) depicts the weld nugget without the addition of the B_4C lubricant to it. The particles were coarse due to the absence of the nucleation effect. Thermally damaged grains are also randomly accessible in the nugget, despite the fact that it contains a fine mix of both copper plates. The coarse grains decreased the ductility of the weld nugget, which resulted in inferior tensile and fatigue characteristics. Figure 6(f), on the other hand, depicts the copper–copper friction stir welding method, which is made possible by B_4C. The grains are finer in size than the B_4C weld nuggets that are not filled. In order to regulate the cooling rate of the boron carbide particle-assisted weld nugget, it is necessary to decrease the development of the copper–copper grain size. The finer grains increased the ductility of the weld nugget, which resulted in better tensile and fatigue characteristics. Grain boundaries are often less thermally impacted than other surfaces because of the lubricating action of the boron carbide particles. Figure 7 reports a scanning electron microscope (SEM) images for the weld sample fabricated with the addition on 3 wt% of B_4C particles. Figure 7(a) shows the SEM image of the base copper alloy. The grain's lamellar structure lends it a surprising amount of elasticity and flexibility. Figure 7(b) depicts the interface layer of the C1100 copper that has been helped by B_4C. The grains have been refined at the interface, and projecting weld patches may be seen in a few places where they meet. The temperature of the interface zone fluctuates as a result of the weld patch variations. Similarly, Figure 7(c) depicts B_4C fine dispersion, which helps explain why the matrix has a finer dispersion than expected. This illustration shows the boron carbide particles enclosed inside the weld nugget in Figure 7(d). The high pore void volume of B_4C particles allows for better heat transmission and lubrication during

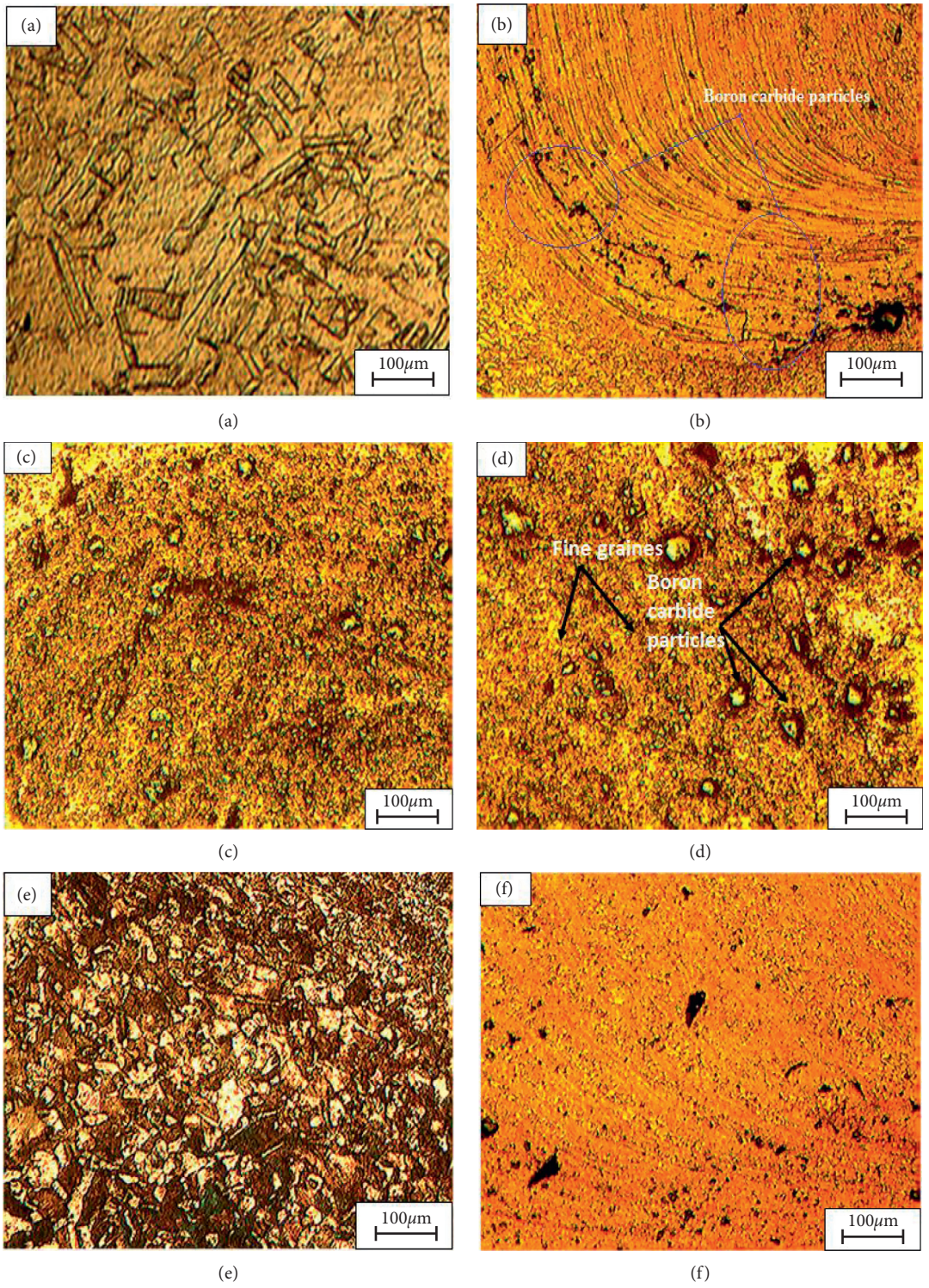

Figure 6: (a) Microstructure of the base copper material. (b–d) Copper-copper interface region and nugget zone inclusion of 3wt% of B_4C particles. (e) Copper-copper nugget zone without B_4C particles added. (f) Low amount of filled B_4C at nugget zone.

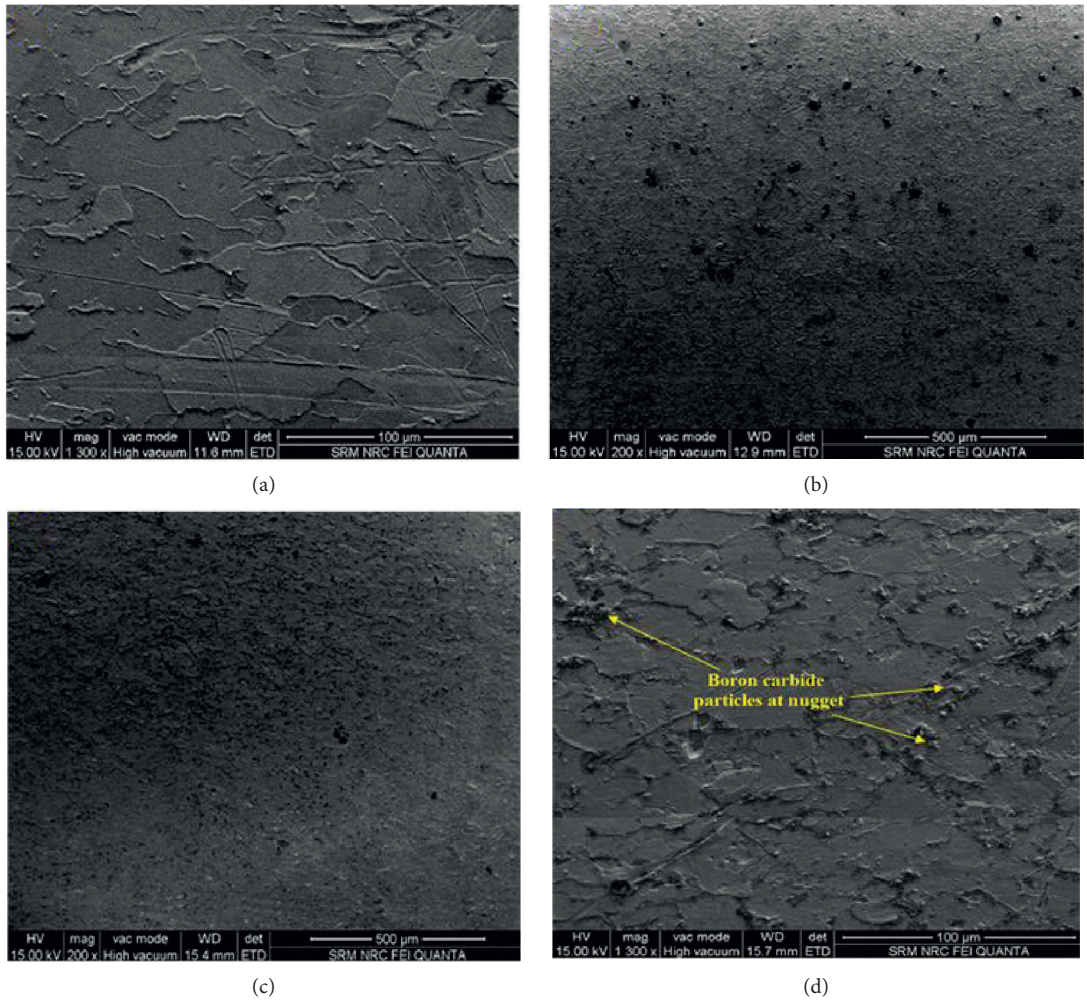

Figure 7: (a) SEM image of base copper. (b–d) SEM images of 3wt% B_4C-assisted welds.

welding because of their large pore void volume. The carbon particles are generated by either an interstitial solution of copper with carbon reinforcement or a solid solution of copper with carbon reinforcement. More to this, the peak is more prominent, suggesting the presence of additional carbon atoms in the boron carbide particles.

7. Conclusions

The novel friction stir welding method was used in this research to create high-quality, thermal stress-sound weld joints with inclusions of boron carbide particles. A high-precision vertical milling machine was utilized to fabricate the weld joints with the recommended process parameters. The following is a summary of the findings of this B_4C-assisted procedure generated from the current research. The inclusion of B_4C particles in the weld zone of C1100 copper and copper was accomplished using a simple butt joint format with a deep drill hole for reinforcement insertion.

(i) With a specific set of process parameters, defect-free and high-quality weld connections were obtained. The specified process parameters had a substantial impact on the weld joint quality, e.g., welding speed, tool rotational speed, axial load, and addition wt% in B_4C particles. The suggested process parameters were chosen to enhance the stress flow of plasticized copper and B_4C particles during the joining process.

(ii) The boron carbide particles polished the copper grains because of their pinning effect. There were no cavities or reaction products at the interface between the B_4C particles and the copper matrix. In the absence of porosity, it is possible to credit this to appropriate weldability between copper and B_4C particles as well as sufficient flow of plasticized copper during FSW at the given set of process parameters.

(iii) The mechanical properties of B_4C-assisted friction stir welding considerably enhanced at 3wt% B_4C addition. The frictional heat is created and distributed across to the B_4C particles throughout the weld zone, resulting in the flow of plasticized copper being sufficient to reveal that defectless weld joints were achieved. The tensile properties are reduced beyond 3 wt% to 4 wt% addition of B_4C particles in the nugget zone. The maximum

tensile and yield strength of C-C3 weld are 203 MPa and 179 MPa, respectively.

(iv) The yield strength and percentage elongation are greater when 3wt% of B_4C is used in the weld zone. Extension and yield strength were both decreased by up to 4% by weight in the presence of additional additives.

(v) The nugget region seems to have the greatest Vickers hardness of B_4C-assisted FSW when compared to the surrounding areas. The hardness of the TMT and HAZ remained considerably lower than that of the nugget. On the other hand, B_4C-assisted welding maintains lower hardness at the nugget and TMT. In the weld zone, the difference in micro-hardness was found to be linked to a change in the distribution and actual volume of B_4C. When B_4C particles were added at a concentration of 3wt%, the highest micro-hardness of 123 HV was achieved.

(vi) B_4C-assisted friction stir welding demonstrates a significant increase in fatigue strength. The C-C3 weld pattern has the maximum fatigue strength of 159 MPa.

(vii) For boron carbide-assisted friction stir-welded nuggets, the microstructure displays a highly processed and finer grain structure, whereas for the unfilled friction stir welding, the grain size is coarser.

(viii) As a result, adding B_4C nanoparticles to the stir region in the process of creating high-quality comparable weld joints may increase the quality of the weld nuggets with a cost-effective pattern. However, boron carbide addition may be beneficial in high-strength metal joining processes such as friction welding and friction stir welding.

Data Availability

The data used to support the findings of this study are included in the article.

Conflicts of Interest

The authors declare that there are no conflicts of interest regarding the publication of this article.

References

[1] M. S. Vetrivel, K. Giridharan, D. P. Pushpanathan et al., "Microstructural and mechanical behaviors of friction stir welded dissimilar aa6082-aa7075 joints," *Advances in Materials Science and Engineering*, vol. 2021, Article ID 4113895, 13 pages, 2021.

[2] G. Karrar, A. Galloway, A. Toumpis, H. Li, and F. Al-Badour, "Microstructural characterisation and mechanical properties of dissimilar AA5083-copper joints produced by friction stir welding," *Journal of Materials Research and Technology*, vol. 9, no. 5, Article ID 11979, 2020.

[3] M. M. Abd Elnabi, A. B. Elshalakany, M. M. Abdel-Mottaleb, T. A. Osman, and A. El Mokadem, "Influence of friction stir welding parameters on metallurgical and mechanical properties of dissimilar AA5454-AA7075 aluminum alloys," *Journal of Materials Research and Technology*, vol. 8, no. 2, pp. 1684–1693, 2019.

[4] A. Eyvazian, F. Hamouda, A. Hamouda, F. Tarlochan, H. A. Derazkola, and F. Khodabakhshi, "Simulation and experimental study of underwater dissimilar friction-stir welding between aluminium and steel," *Journal of Materials Research and Technology*, vol. 9, no. 3, pp. 3767–3781, 2020.

[5] T. Sathish, V. Mohanavel, and A. Karthick, "Study on Compaction and machinability of silicon nitride (Si3N4) reinforced copper alloy composite through P/M route," *International Journal. Polymer Science*, vol. 2021, Article ID 7491679, 10 pages, 2021.

[6] H. Khodaverdizadeh, A. Heidarzadeh, and T. Saeid, "Effect of tool pin profile on microstructure and mechanical properties of friction stir welded pure copper joints," *Materials & Design*, vol. 45, pp. 265–270, 2013.

[7] S. R. Narasimharaju and S. Sankunny, "Microstructure and fracture behavior of friction stir lap welding of dissimilar AA 6060-T5/Pure copper," *Engineering Solid Mechanics*, vol. 7, pp. 217–228, 2019.

[8] G. R. Joshi, "Studies on Tool Shoulder Diameter of Dissimila Friction Stir Welding Copper to Stainless Steel," *Metallography, Microstructure, and Analysis*, vol. 8.

[9] S. Emami, S. Sadeghi-Kanani, T. Saeid, and F. Khan, "Dissimilar friction stir welding of AISI 430 ferritic and AISI 304L austenitic stainless steels," *Archives of Civil and Mechanical Engineering*, vol. 20, no. 131, 2020.

[10] A. T. Nia and A. Ali, "Investigating the properties of bimetallic aluminum -clad copper tubes produced by friction stir welding," *Journal of Alloys and Compounds*, vol. 751, pp. 299–306, 2018.

[11] K. P. Metha, "Badheka VJ"Hybrid approaches of assisted heating and cooling for friction stir welding of copper to aluminum joints," *Journal of Materials Processing Technology*, vol. 239, pp. 336–345, 2017.

[12] T. Sathish, V. Mohanavel, and A. Karthick, "Study on Compaction and machinability of silicon nitride (Si_3N_4) reinforced copper alloy composite through P/M route," *International Journal of Polymer Science*, vol. 2021, Article ID 7491679, 10 pages, 2021.

[13] V. C. Sinha, S. Kundu, and S. Chatterjee, "Microstructure and mechanical properties of similar and dissimilar joints of aluminium alloy and pure copper by friction stir welding," *Perspectives in Science*, vol. 8, pp. 543–546, 2016.

[14] P. Sevvel, C. Satheesh, and V. Jaiganesh, "Influence of tool rotational speed on microstructural characteristics of dissimilar Mg alloys during friction stir welding," *Transactions of the Canadian Society for Mechanical Engineering*, vol. 43, no. 1, pp. 132–141, 2019.

[15] M. Jafari, M. Abbasi, D. Poursina, A. Gheysarian, and B. Bagheri, "Microstructures and mechanical properties of friction stir welded dissimilar steel-copper joints," *Journal of Mechanical Science and Technology*, vol. 31, no. 3, pp. 1135–1142, 2017.

[16] P. M. G. P. Moreira, T. Santos, S. M. O. Tavares, V. R. Trummer, P. Vilaça, and P. M. S. T. D. Castro, "Mechanical and metallurgical characterization of friction stir welding joints of aa6061-T6 with aa6082-T6," *Materials & Design*, vol. 30, no. 1, pp. 180–187, 2009.

[17] E. G. Cole, A. Fehrenbacher, N. A. Duffie, M. R. Zinn, F. E. Pfefferkorn, and N. J. Ferrier, "Weld temperature effects

during friction stir welding of dissimilar aluminum alloys 6061-t6 and 7075-t6," *International Journal of Advanced Manufacturing Technology*, vol. 71, no. 1-4, pp. 643–652, 2014.

[18] B. Gungor, E. Kaluc, and E. Taban, "Mechanical, Fatigue and microstructural properties of friction stir welded 5083-H111 and 6082-T651 aluminum alloys," *Materials and Design (1980-2015)*, vol. 56, pp. 84–90, 2014.

[19] P. Niu, W. Li, X. Yang, and A. Vairis, "Effects of microstructural asymmetries across friction stir welded AA2024 joints on mechanical properties," *Science and Technology of Welding & Joining*, vol. 23, no. 1, pp. 58–62, 2018.

[20] H. J. Liu, J. J. Shen, L. Zhou, Y. Q. Zhao, C. Liu, and L. Y. Kuang, "Microstructural characterisation and mechanical properties of friction stir welded joints of aluminium alloy to copper," *Science and Technology of Welding & Joining*, vol. 16, no. 1, pp. 92–98, 2011.

[21] P. K. Vijaya, G. R. Madhusudhan, and K. R. Srinivasa, "Microstructure and pitting corrosion of armor grade AA7075 aluminum alloy friction stir weld nugget zone - effect of post weld heat treatment and addition of boron carbide," *Defence Technology*, vol. 11, no. 2, pp. 166–173, 2015.

[22] O. Zareie, S. M. Mousavizade, H. R. Ezatpour, H. Zareie, and N. Farmanbar, "Effect of plunging depth and dwelling time on microstructure and mechanical properties of 6061 aluminum alloy welded by protrusion friction stir spot welding," *Welding in the World*, vol. 64, 2020.

[23] A. Al-Shahrani, "Wynne BP "Effect of dwell time on friction stir spot welded dual phase steel," *Advanced Materials Research*, vol. 83, pp. 1143–1150, 2010.

[24] P. Sevvel and V. Jaiganesh, "Influence of the arrangement of materials and microstructural analysis during FSW of AZ80A & AZ91C Mg alloys," *Archives of Metallurgy and Materials*, vol. 62, no. 3, pp. 1795–1801, 2017.

[25] H. A. Derazkola and M. Elyasi, "Hossienzadeh M "Effects of friction stir welding tool plunge depth on microstructure and texture evolution of AA1100 to A441 AISI joint," *International Journal of Advanced Design and Manufacturing*, vol. 9, no. 1, 2016.

[26] "Rajadurai A"Thermo-mechanical characterization of siliconized E-glass fiber/hematite particles reinforced epoxy resin hybrid composite," *Applied Surface Science*, vol. 384, pp. 99–106, 2016.

[27] T. Medhi, B. S. Roy, and S. C. Saha, "An experimental investigation on the influence of rotational speed on microstructure and mechanical properties of friction stir welded dissimilar Al-Cu joints," *International Journal of Materials and Product Technology*, vol. 60, no. 2-4, pp. 236–259, 2020.

[28] G. Güleryüz, "Relationship between FSW parameters and hardness of the ferritic steel joints: modeling and optimization," *Vacuum*, vol. 178, Article ID 109449, 2020.

[29] P. Sevvel and V. Jaiganesh, "Effect of tool shoulder diameter to plate thickness ratio on mechanical properties and nugget zone characteristics during FSW of dissimilar Mg alloys," *Transactions of the Indian Institute of Metals*, vol. 68, no. S1, pp. 41–46, 2015.

[30] D. Texier, F. Atmani, P. Bocher et al., "Fatigue performances of FSW and GMAW aluminum alloys welded joints: competition between microstructural and structural-contact-fretting crack initiation," *International Journal of Fatigue*, vol. 116, pp. 220–233, 2018.

[31] E. Cetkin, Y. H. Çelik, and S. Temiz, "Microstructure and mechanical properties of AA7075/AA5182 jointed by FSW," *Journal of Materials Processing Technology*, vol. 268, pp. 107–116, 2019.

[32] R. Sathishkumar, N. Murugan, I. Dinakaran, and S. J. Vijay, "Role of friction stir processing parameters on microstruture and microhardness of boron carbide particulate reinforced copper surface composites," *Sadhana*, vol. 38, 2013.

[33] R. Sathishkumar, N. Murugan, I. Dinakaran, and S. J. Vijay, "Effect of traverse speed on microstruture and microhardness of cu/B_4C surface composite produced by friction stir processing," *Transactions of the Indian Institute of Metals*, vol. 66, no. 4, pp. 333–337, 2013.